Study of Rydberg-atom l-changing collisions using selective field ionization

F. G. Kellert,* T. H. Jeys, G. B. McMillian, K. A. Smith, F. B. Dunning, and R. F. Stebbings

Space Physics and Astronomy Department and the Rice Quantum Institute, Rice University, Houston, Texas 77001
(Received 14 July 1980)

The excited products of collisions between xenon atoms and Na(nd) atoms with $n = 37$ and $n = 42$ have been investigated by use of selective field ionization (SFI). It is observed that, at an ionizing-field slew rate of $\sim 10^9$ V/cm sec, most of the collision products follow predominantly diabatic paths to ionization which occurs at field strengths consistent with those predicted by quantum mechanical tunneling calculations. Detailed analysis of the SFI data indicates that the collision products have a wide (possibly complete) range of values of l and m_j, although it is not clear whether the observed distribution results from single or multiple collisions. No evidence of n-changing collisions was seen. Similar data for collisions involving Xe(nf) atoms are briefly discussed.

I. INTRODUCTION

Collisions involving a Rydberg atom in a state of principal quantum number n, and angular momentum quantum number l can result *inter alia* in "l-changing" reactions. Such collisions have been previously studied for a variety of collision partners using selective field ionization (SFI).[1-7]

In the present work the excited products resulting from Na(nd)-Xe collisions have been investigated for $n = 37$ and 42. The measured SFI profiles are interpreted with the aid of model calculations based on current theories of field ionization.

II. EXPERIMENTAL TECHNIQUE

The apparatus has been described elsewhere[8] and is shown schematically in Fig. 1. Sodium atoms are excited, in zero (≤ 0.2 V cm^{-1}) electric field, to selected $nd(^2D_{3/2, 5/2})$ Rydberg states by laser induced, two-step photoexcitation via the intermediate $3\,^2P_{3/2}$ state. The excitation region is located between two fine-mesh, planar, parallel grids. To study the effects of collisions xenon is introduced into the apparatus at a pressure of $\sim 10^{-4}$ Torr.

The laser-excited atoms, and the excited collision products, are detected and analyzed by use of SFI for which purpose a pulsed electric field is applied ~ 10 μsec after excitation across the collision region. This field, which rises from 0 to ~ 1000 V cm^{-1} in ~ 1 μsec, is generated by application of a voltage ramp across the two parallel grids. The electrons liberated at ionization are detected by an electron multiplier whose output is fed to a time-to-amplitude converter (TAC). The TAC is started at the beginning of the ionizing voltage ramp and is stopped by the first electron pulse subsequently registered by the detector. The TAC output is fed into a standard multichannel pulse analyzer. For sufficiently low count rates (less than 0.1 per laser pulse) the multichannel analyzer stores a signal proportional to the probability of a field ionization event per unit time during the 1 μsec ramp. Knowledge of the time dependence of the ionizing field strength then allows the probability of field ionization per unit field increment to be derived.

Since atoms in different Rydberg states ionize at different electric field strengths, it is in principle possible to infer from SFI data the state distribution of the excited reaction products. However, such an analysis clearly requires an understanding of how these atoms respond as the applied field is increased from zero to the value at which ionization occurs. Difficulty is encountered here in that the atoms are excited, in zero field, to states that, neglecting nuclear spin, are described by the quantum numbers n, l, j, and m_j. When these atoms are exposed to an increasing electric field, various internal couplings are broken and the quantum numbers l, j, and m_j lose their meaning. At high fields the parabolic quantum numbers n, n_1, n_2, and $|m_l|$ together with m_s provide a better description[9] and the behavior at ionization is best discussed with reference to these quantum numbers.

Evidently then, one needs to understand how atoms initially in states (n, l, j, and m_j) evolve under an increasing electric field into (n, n_1, n_2,
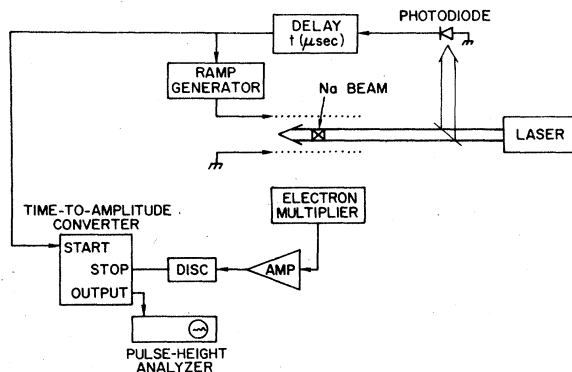

FIG. 1. Schematic diagram of the apparatus.

and $|m_l|$) states. In this regard it is to be noted that at all field strengths the component of the total angular momentum along the field axis is conserved, i.e., $m_j = m_l + m_s$.

As will be discussed, the value of $|m_l|$ is very important in determining the ionization threshold of an atom and since we may write

$$|nljm_j\rangle = \sum_{m_l m_s} a_{m_l m_s} |nlm_l m_s\rangle ,$$

where the $a_{m_l m_s}$ are Clebsch-Gordan coefficients, it is evident that a given $|n, l, j, m_j\rangle$ state may correlate with Stark states having more than one value of $|m_l|$ and may thus exhibit more than one ionization threshold.

III. FIELD IONIZATION

Field ionization has been discussed in detail by several authors[8,10-15] and only a brief review of its essential features will be included here. The process will be discussed by reference to Fig. 2 which shows, as a function of electric field, the energy of the $m_l = 0$ Stark states of hydrogen in the vicinity of $n = 15$, calculated by use of fourth-order perturbation theory.[16,17] As illustrated in the inset in Fig. 2 the application of an electric field creates a saddle point in the potential seen by the Rydberg electron. The line labeled V_{sad} shows the height of this saddle point as a function of the applied electric field strength and separates the region, on the right, within which ionization is classically possible from that where it is not. However, the effective potential energy of the Rydberg electron includes a centrifugal term due to its angular momentum about the z axis.[18] For a given excitation energy, states of higher $|m_l|$ require higher fields to ionize. The line labeled V_{sad} in Fig. 2 applies to $m_l = 0$ states.

In quantum mechanical treatments of field ionization the electron may escape from the atom by tunneling [quantum mechanical tunneling, (QMT)] and the various hydrogenic Stark states shown in Fig. 2 have appreciable ionization rates ($>10^7$ sec^{-1}) only in the dashed regions.[19] It is evident from Fig. 2 that quantum mechanical treatments lead to the result that, within a given manifold, the higher Stark states remain stable in fields for which they are classically unstable. This is readily understood since the high-lying Stark states have wave functions with very little electron probability density in the vicinity of the saddle point,[9] where electron escape may most readily occur, and thus ionization is inhibited. However, the lowest members of each Stark manifold have probability densities that are maximum in the vicinity of the saddle point, and hence attain large ionization rates at the ionization thresholds predicted by classical saddle-point theory.

The response of an atom to high fields is complicated by the presence of non-Coulombic terms in the Hamiltonian. These result in interactions between states of the same $|m_l|$ and, in consequence, avoided crossings occur when states of the same $|m_l|$ in different Stark manifolds approach one another.[17,20] The general Stark structure for sodium atoms is nevertheless similar to hydrogen, except for the presence of avoided crossings where states from different manifolds cross. Their ionization may therefore be discussed using energy levels and ionization rates calculated using relatively simple hydrogenic theory.

The ionization characteristics of an atom are critically dependent on its behavior at avoided crossings. For an atom in a state that is not strongly coupled to other states the energy separation at avoided crossings is small. Then if the applied field is increased sufficiently rapidly there is a high probability that the intermanifold avoided crossings will be traversed diabatically. The atom then remains in a single state following a path to ionization like that shown by the heavy dashed line in Fig.2, and ionization occurs at the quantum mechanical limit. Ionization of $m_l = 0$ states in the $n = 15$ manifold would then occur over the range of field strengths marked "diabatic" in Fig. 2. On the other hand, if the atom is initially
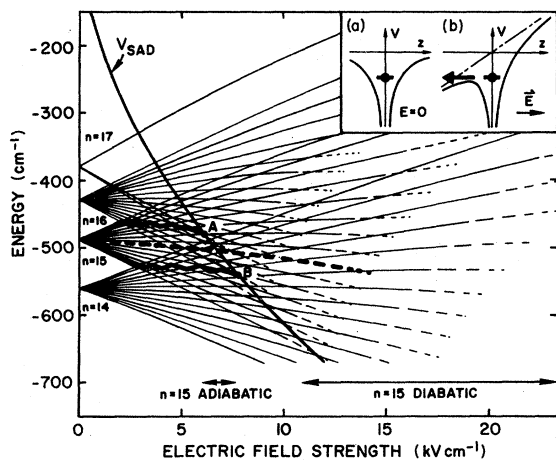

FIG. 2. The $m_l = 0$ Stark states in the vicinity of $n = 15$. The high-field end of each state is dashed to indicate the range of fields over which the ionization rate increases from $\sim 10^7$ to 10^{11} sec^{-1}. The heavy solid lines give examples of adiabatic passage to ionization; the heavy dashed line is an example diabatic passage. In the inset is shown the potential energy of the Rydberg electron in (a) the absence and (b) the presence of an external field directly along the z axis. The height of the resultant saddle point as a function of the applied field is shown by the line labeled V_{sad}.

in a state which interacts strongly with states of other manifolds the energy separations at avoided crossings are large. Then, if the rate of increase, i.e., slew rate, of the electric field is sufficiently slow, there is a high probability that these avoided crossings will be traversed adiabatically. The atom will then follow paths to ionization such as those indicated by the solid lines in Fig. 2, the atom successively assuming the character of many different Stark states. All atoms in $m_l = 0$ states in the $n = 15$ Stark manifold that follow adiabatic paths to ionization cross the $m_l = 0$ saddle-point line V_{sad} between points A and B. To the right of this line the atoms experience a dramatic increase in ionization probability due to their interaction with states of higher Stark manifolds that are highly unstable against ionization in this region. They therefore ionize at field strengths close to those predicted by classical saddle-point theory, i.e., in the range marked "adiabatic" in Fig. 2. An atom may also exhibit a combination of adiabatic and diabatic behavior at curve crossings during passage to ionization.

The intermanifold interactions are highly $|m_l|$ dependent, the larger the value of $|m_l|$ the smaller the interaction between states of the same $|m_l|$ at level crossings.[17] States of higher n also exhibit less interaction at level crossings. Thus the probability of diabatic passage to ionization increases both with $|m_l|$ and with n. For sodium it is found that for atoms with $n \sim 40$, states with $|m_l| \lesssim 1$ ionize predominantly adiabatically, while those with $|m_l| > 1$ ionize predominantly diabatically,[8] at the slew rates used in the present study, (typically $\sim 10^9$ V cm^{-1} sec^{-1}).

IV. RESULTS AND DISCUSSION

A. Data

A typical SFI spectrum obtained for laser-excited Na(37d) atoms, in the absence of target gas, 10 μsec after the laser pulse is shown in Fig. 3(c). Two major ionization features are observed whose origins have been discussed in detail elsewhere.[8]

Briefly the small high-field feature at about 350 V cm^{-1} is attributed to diabatic ionization of states with $|m_l| = 2$. This identification is made because, as is evident from Fig. 3(d), the high-field threshold is consistent with that predicted by QMT calculations for the lowest member of the $n = 37$, $|m_l| = 2$ Stark manifold, which is the $|m_l| = 2$ Stark state resulting from 37d excitation. Supporting this identification is the observation that the size of the high-field feature increased dramatically when the polarization of the exciting lasers was chosen to maximize the production of states with values of m_j
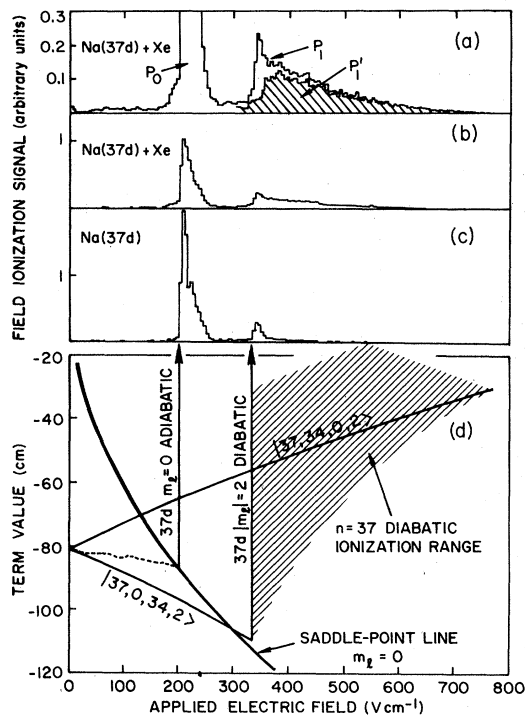

FIG. 3. Interpretation of SFI data. (a) SFI spectrum obtained $\sim 10 \mu$ sec after laser excitation of Na(37d) in the presence of $\sim 10^{-4}$ Torr of xenon. The peak P_1 results from diabatic ionization of both parent and product states with $|m_l| > 1$. The hatched area P_1' represents the contribution due to product states alone. (b) The same spectrum as (a) showing the relative sizes of the P_0 and P_1 features. (c) SFI spectrum obtained $\sim 10 \mu$sec after laser excitation of Na(37d) in the absence of xenon target gas. (d) The dotted line indicates the adiabatic path to ionization of the 37d $m_l = 0$ state. The heavy diverging solid lines show the extreme members of the $|m_l| = 2$ $n = 37$ Stark manifold and are terminated at an ionization rate of 10^9 sec^{-1}. Atoms in $n = 37$ $|m_l| > 1$ Stark states ionize diabatically over the range of field strengths indicated by the cross hatching.

correlating with $|m_l| = 2$. Further, no corresponding high-field feature was evident in the ionization of ns atoms, for which $m_l = 0$. In the present work both lasers were polarized parallel to the ionizing field direction in an attempt to minimize the production of $|m_l| = 2$ states. Under these conditions no signal due to $|m_l| = 2$ states should, in principle, be observed. A small signal due to $|m_l| = 2$ states is, however, observed and is attributed to the effects of small ($\lesssim 0.2$ V cm^{-1}) residual electric fields in the interaction region.

The low-field feature at around 200 V cm^{-1}, is attributed to ionization along predominantly adiabatic paths. The adiabatic path to ionization for the $m_l = 0$ state resulting from 37d excitation is shown by the dashed line in Fig. 3(d). The electric

field strength at which this intersects the $m_l = 0$ saddle-point line is in good agreement with the experimentally determined low-field ionization threshold. The low-field ionization feature also encompasses the predicted threshold for adiabatic ionization of the $|m_l| = 1$ states resulting from $37d$ excitation. Thus this feature is attributed to predominantly adiabatic ionization of $|m_l| = 0$ and 1 states.

Figures 3(a) and 3(b) show, on different scales, the SFI spectrum observed after laser-excited $Na(37d)$ atoms have been allowed to interact for 10 μsec with Xe target gas. An important feature of this spectrum is that ionization is observed at fields greater than those associated with ionization of laser-excited $|m_l| = 2$ states. All the atoms that ionize at critical electric fields equal to or greater than those for laser-excited $|m_l| = 2$ states comprise the feature labeled P_1. A small signal on the low-field side of the parent $37d$ adiabatic feature is also evident. Further, some of the collision products ionize between the adiabatic and diabatic thresholds. The interpretation and origin of the collisionally produced features evident in the SFI spectrum are discussed in the following sections.

B. SFI data analysis: The P_1 feature

The P_1 feature in Fig. 3a results from diabatic ionization of both parent $|m_l| = 2$ atoms and of atoms resulting from collisions with the xenon target gas. The portion of P_1 that results from the collision products can be identified by subtraction from P_1 of the contribution due to the remaining parent atoms.[21] The resultant profile, labeled P_1', is included in Fig. 3a. As evident from Fig. 3d, the position and width of the P_1' feature corresponds to that expected for diabatic ionization, at the QMT limit, of a mixture of all $n = 37$ $|m_l| > 1$ Stark states. Information on the identity of the states of the atoms comprising P_1' can be obtained by comparing the experimental P_1' profile with those calculated for ionization of different assumed mixtures of product states at the QMT limit. These profiles are calculated in the following manner.

Consider a ramped ionizing electric field F_t that begins at time t_0. If $N(t_0)$ atoms are present at t_0 in a particular Stark state and if the ionization probability is $I(F_t)$, then at a later time t, the number $N(t)$ of atoms remaining is given by

$$N(t) = N(t_0) \exp\left(-\int_{t_0}^{t} I(F_t)\, dt\right). \tag{1}$$

Since the field changes in time, the ionization probability $I(F_t)$ is implicitly time dependent. The measured field ionization signal $ds(t)/dt$ corresponds to the number of electrons liberated by field

ionization per unit time, and is given by

$$\frac{ds(t)}{dt} = I(F_t)N(t)$$

$$= N(t_0)I(F_t) \exp\left(-\int_{t_0}^{t} I(F_t)\, dt\right). \tag{2}$$

Knowledge of the electric field strength as a function of time, and the corresponding ionization rate, calculated by use of the procedure of Damburg and Kolosov,[19] allows $I(F_t)$ and thence the SFI profile to be calculated. The total field ionization signal appropriate to a mixture of states can be calculated by summing the separate contributions due to each state, weighted by the initial population in each state.

For example, the profile shown in Fig. 4b is that calculated for diabatic ionization, at a slew rate of 10^9 V cm^{-1} sec^{-1}, of a mixture containing equal numbers of atoms in each $|m_l| > 1$ Stark state for $n = 37$. For purposes of illustration the extreme members of the $|m_l| = 2$ Stark manifold are shown in Fig. 4a together with a series of points each of which represents the location at which one of the $|m_l| > 1$ Stark states achieves an ionization rate of 10^9 sec^{-1}. A detailed comparison between this calculated profile and the experimental P_1' data is shown in Fig. 5b. The two profiles are normalized to have equal areas. The good agreement between them suggests that the P_1' feature results from
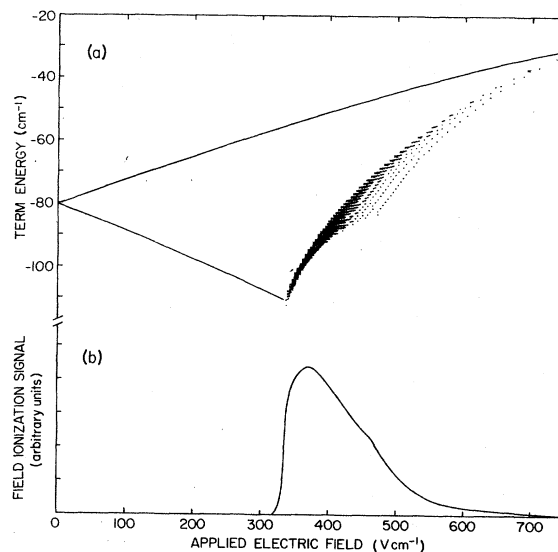

FIG. 4. (a) Extreme members of the $n = 37$ $|m_l| = 2$ Stark manifold. The crosses represent the points at which each $|m_l| > 1$ Stark state achieves an ionization rate of 10^9 sec^{-1}. (b) Calculated SFI profile for diabatic ionization of a mixture containing equal numbers of atoms in each $|m_l| > 1$ Stark state for $n = 37$ at a slew rate of 10^9 V cm^{-1} sec^{-1}.

ionization of a statistically distributed $n = 37$ population at the QMT limit, although the calculated profiles are in fact somewhat insensitive to the exact choice of the maximum and minimum values of $|m_l|$ employed in the summation. SFI studies of the products of Na(42d)–Xe collisions yielded the P_1' feature shown in Fig. 5a. The position and profile of this feature is again consistent with that calculated for diabatic ionization of the QMT limit of the $|m_l| > 1$ states present in a statistically distributed population of $n = 42$ atoms. Thus SFI data indicate that collisions, which occur in near zero field, result in the production of an ensemble of atoms that when subjected to a high electric field evolve into a wide (perhaps statistical) distribution of Stark states. From this it may be inferred that this ensemble has a wide, possibly complete, range of values of l, j. and m_j, although it remains to be determined whether this distribution results directly from single collisions, or from multiple collisions. This result is consistent with earlier work[1] concerning Na(17d)–Ar collisions in which the absence of selection rules on the changes in l and $|m_l|$ resulting from collisions was also noted.

C. SFI data analysis: Other collision-induced SFI features

The small collisionally induced SFI feature evident in Figs. 3(a) and 3(b) on the low-field side of the parent adiabatic feature is attributed to the adiabatic ionization of the products of reactions that yield Stark states with $|m_l| \leq 1$. Adiabatic ionization is modeled by tracing the path of each $|m_l| \leq 1$ state, as the field is increased, through avoided crossings with states from othe manifolds. The atom is assumed to successively take on the char-

acter of each state comprising this path. This process is continued until at sufficiently high fields the state of interest undergoes an avoided crossing with a state that is unstable against ionization. At such an avoided crossing the atom assumes the character of the ionizing state and ionization will occur. The field ionization signal due to each initial state is computed for Eq.(2) using the values of $I(F_t)$ appropriate to the various states comprising the adiabatic path. The total field ionization signal resulting from adiabatic ionization of a mixture of initial Stark states is then obtained by summing the separate contributions from each initial state.

The SFI profile calculated for adiabatic ionization of a mixture containing equal numbers of atoms in each $n = 37$, $|m_l| \leq 1$ Stark state is shown in Fig. 6 which also includes the profile for diabatic ionization of the l-mixed collision products with $|m_l| > 1$ together with representative SFI data. The areas under the calculated adiabatic and diabatic profiles are in the ratio of the number of atoms in a completely mixed $n = 37$ population with $|m_l| \leq 1$ to the number with $|m_l| > 1$. It is evident from Fig. 6 that the small collisionally induced SFI feature on the low-field side of the parent peak can be correlated with the adiabatic ionization of the low $|m_l|$ collision products.

Inspection of Figs. 3 and 6, shows that a very small fraction of the collisionally induced product atoms ionize in the region between the adiabatic and diabatic features. This signal may result from reaction products that have followed partially diabatic and partially adiabatic paths to ionization and ionize in the region beyond the appropriate saddle-point critical field loci as a result of coupling to other states. However, the present data indicate that an overwhelmingly large fraction of the state changed atoms either ionize along predominantly adiabatic paths or follow predominantly diabatic paths to high fields and ionize at field strengths consistent with those predicted by QMT calculations.

No collisionally induced ionization features are detected at field strengths below those required to ionize atoms in states with the same principal quantum number as the parent state. This demonstrates that collisions of Na(nl) with xenon do not significantly populate states of higher n. From this we infer that there is no significant collisional population of states with lower n.
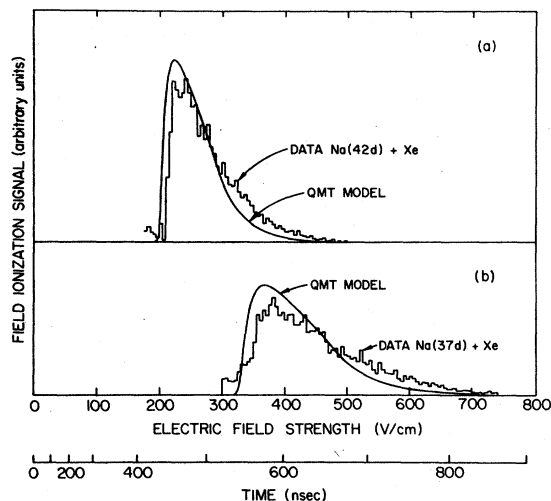

FIG. 5. Detailed comparison of the calculated and observed P_1' profiles for $n = 42$ and $n = 37$.

V. STUDIES INVOLVING OTHER RYDBERG SPECIES

SFI has also been applied in this laboratory to the investigation of collisions involving Xe(nf) Rydberg atoms. Interactions with the target gases
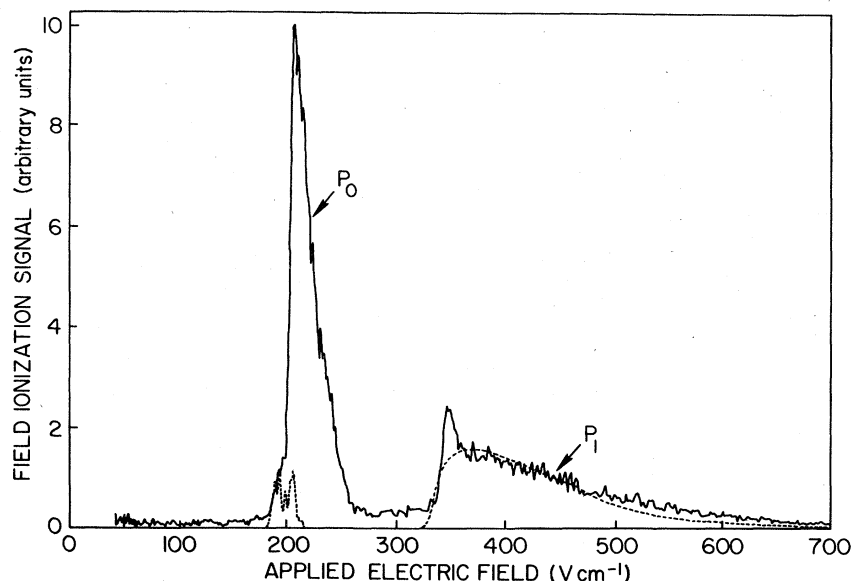
FIG. 6. Calculated ionization features(---) resulting from ionization of a mixture containing equal numbers of atoms in each $n = 37$ Stark state. States with $|m_l| \leq 1$ ionize adiabatically resulting in the feature at ~ 200 V cm^{-1}; states with $|m_l| > 1$ ionize diabatically at fields in the range ~ 330–750 V cm^{-1}. For comparison purposes typical SFI data obtained following Na$(37d)$-Xe collisions are included.

SF_6 and Xe result in the appearance of a P_1' feature similar to that observed following Na(nd)-Xe interactions. Detailed analysis of the position and profile of the P_1' features again indicates that l-changing collisions yield products in a wide range of quantum states.

The present data show that a moderately detailed analysis of collisional processes is possible through comparisons between observed and calculated SFI profiles. This technique is now being applied to study n and l changing in collisions involving a wide variety of polar targets.

ACKNOWLEDGMENTS

*Present address: Optoelectronics Division, Hewlett-Packard, 640 Page Mill Road, Palo Alto, California 94304.

[1]T. F. Gallagher, W. E. Cooke, and S. A. Edelstein, Phys. Rev. A 17, 904 (1978).

[2]K. A. Smith, F. G. Kellert, R. D. Rundel, F. B. Dunning, and R. F. Stebbings, Phys. Rev. Lett. 40, 1362 (1978).

[3]F. G. Kellert, K. A. Smith, R. D. Rundel, F. B. Dunning, and R. F. Stebbings, J. Chem. Phys. 72, 3179 (1980).

[4]K. B. MacAdam, D. A. Crosby, and R. Rolfes, Phys. Rev. Lett. 44, 980 (1980).

[5]F. G. Kellert, C. Higgs, K. A. Smith, G. F. Hildebrandt, F. B. Dunning, and R. F. Stebbings, J. Chem. Phys. 72, 6312 (1980).

[6]R. F. Stebbings, F. B. Dunning, and C. Higgs, J. Electron Spectrosc. Relat. Phenom. (in press).

[7]C. Higgs, K. A. Smith, G. B. McMillian, F. B. Dunning, and R. F. Stebbings, J. Phys. B (in press).

[8]T. H. Jeys, G. W. Foltz, K. A. Smith, E. J. Beiting, F. G. Kellert, F. B. Dunning, and R. F. Stebbings, Phys. Rev. Lett. 44, 390 (1980).

[9]H. A. Bethe and E. E. Salpeter, Quantum Mechanics of One- and Two-Electron Atoms (Springer, Berlin, 1957).

[10]M. G. Littman, M. L. Zimmerman, and D. Kleppner, Phys. Rev. Lett. 37, 486 (1976).

[11]T. F. Gallagher, L. M. Humphrey, R. M. Hill, and S. A. Edelstein, Phys. Rev. Lett. 37, 1465 (1976).

[12]T. F. Gallagher, L. M. Humphrey, W. E. Cooke, R. M. Hill, and S. A. Edelstein, Phys. Rev. A 16, 1098 (1977).

[13]T. F. Gallagher and W. E. Cooke, Phys. Rev. A 19, 694 (1979).

[14]J. L. Vialle and H. T. Duong, J. Phys. B 12, 1407 (1979).

[15]M. G. Littman, M. M. Kash, and D. Kleppner, Phys. Rev. Lett. 41, 103 (1978).

[16]H. J. Silverstone, Phys. Rev. A 18, 1853 (1978).

[17]M. L. Zimmerman, M. G. Littman, M. M. Kash, and D. Kleppner, Phys. Rev. A **20**, 2251 (1979).

[18]W. E. Cooke and T. F. Gallagher, Phys. Rev. A **17**, 1226 (1978).

[19]R. J. Damburg and V. V. Kolosov, J. Phys. B **9**, 3149 (1976); Phys. Lett. **61A**, 233 (1977); Opt. Commun. **24**, 211 (1978); J. Phys. B **12**, 2637 (1979). See also, M. H. Rice and R. H. Good, Jr., J. Opt. Soc. Am. **52**, 239 (1962); D. S. Bailey, J. R. Hiskes, and A. C. Riviere, Nucl. Fusion **5**, 41 (1965); D. R. Herrick, J. Chem. Phys. **65**, 3529 (1976).

[20]M. G. Littman, M. L. Zimmerman, T. W. Ducas, R. R. Freeman, and D. Kleppner Phys. Rev. Lett. **36**, 788 (1976).

[21]Let $C(j)$ equal the number of counts in the jth channel of the multichannel analyzer. If $C_{in}(j)$ and $C_{out}(j)$ represent counts recorded in the presence and absence of target gas, respectively, and if the ratio of adiabatically ionizing atoms with and without target gas is R, then the signal resulting from diabatic ionization of collision products is taken to be $C_{diff}(j) = C_{in}(j) - RC_{out}(j)$. This procedure assumes that only a small fraction of the collision products ionize adiabatically and that the laser-excited Na(nd) atoms undergo state-changing collisions regardless of the initial value of $|m_l|$, namely, 0, 1, or 2.